



Fractional order mathematical model for B.1.1.529 SARS-Cov-2 Omicron variant with quarantine and vaccination

S. Dickson¹ · S. Padmasekaran¹ · Pushpendra Kumar²

Received: 2 January 2023 / Revised: 4 February 2023 / Accepted: 13 February 2023 / Published online: 7 March 2023
© The Author(s), under exclusive licence to Springer-Verlag GmbH Germany, part of Springer Nature 2023

Abstract

In this paper, a fractional order nonlinear model for Omicron, known as B.1.1.529 SARS-Cov-2 variant, is proposed. The COVID-19 vaccine and quarantine are inserted to ensure the safety of host population in the model. The fundamentals of positivity and boundedness of the model solution are simulated. The reproduction number is estimated to determine whether or not the epidemic will spread further in Tamilnadu, India. Real Omicron variant pandemic data from Tamilnadu, India, are validated. The fractional-order generalization of the proposed model, along with real data-based numerical simulations, is the novelty of this study.

Keywords Omicron · Stability · Reproduction number · Steady states · Fractional derivative

Mathematics Subject Classification 26A33 · 34A08 · 65P40

1 Introduction

As of November 24, 2021, Omicron has been found in several nations and was still the dominant variety everywhere. Omicron infection results in a less serious illness than infection with the earlier forms. Omicron may cause a milder form of disease, according to preliminary research, but some people who acquire this variant's infection still run the risk of developing serious illness, needing hospitalization, and even passing away. One should take precautions even if only a tiny portion of those with Omicron infection require hospitalization because the high incidence of cases could collapse the healthcare system. The Omicron variation, also known as

B.1.1.529 SARS-Cov-2 Variant, was less contagious than the original COVID-19 virus and the Delta variant. People who have the Omicron variant infection may exhibit symptoms that are similar to those of earlier forms. For an individual, experienced a prior infection, received a COVID-19 vaccination, and the existence of other health issues can all affect the presence and intensity of symptoms. The most effective public health measure for preventing COVID-19 and reducing the possibility of new variations arising is still COVID-19 vaccination. This covers the initial course, booster shots, and any necessary subsequent doses. It is anticipated that the current vaccines will guard against the serious sickness, hospital stays, and fatalities brought on by Omicron variant infection. Breakthrough infections in vaccinated people are also likely.

Several mathematical models have been developed in a wide range of manners to describe how diseases spread in sub-population compartments. In [1], the authors proposed a nonlinear model for the co-dynamics of tuberculosis and COVID-19. In [2], the authors modeled the spatial distribution of a COVID-19 with vaccination using a diffusion equation. In [3], the researchers proposed a novel delay-type model of COVID-19 with a convex incidence rate. The authors in [4] simulated the impact of quarantine and hospitalization on the transmission of COVID-19. In Peter et al. [5], proposed a novel model of COVID-19 using real data from Pakistan. In [6], the authors proposed a non-

All authors have contributed equally to this work.

✉ S. Padmasekaran
padmasekarans@periyaruniversity.ac.in

S. Dickson
dickson@periyaruniversity.ac.in

Pushpendra Kumar
kumarsaraswatpk@gmail.com; pkkumar@uj.ac.za

¹ Mathematics, Periyar University, Periyar Palakalainagar, Salem, Tamilnadu 636011, India

² Institute for the Future of Knowledge, University of Johannesburg, P.O. Box 524, Auckland Park 2006, South Africa

linear model of COVID-19 for studying the outbreaks in Nigeria with optimal controls. The Omicron variant is challenging mathematicians to rethink models that have aided India’s comprehension of COVID-19 and response to the outbreak. With the next wave of the pandemic, everyone from those who get tested to whom most likely to get the virus has altered, providing new hurdles for those who model its impact. The vaccine class has been considered in the models, which allows appropriate antibodies to be supplied to the recovered and powerless persons in the host population when a wiped out individual recovers from an illness [7–9]. Asymptotic strong characteristics move from the infection free consistent state to the endemic consistent state. Because there are no known numerical approaches for developing Lyapunov capabilities for epidemic models, investigating the global aspects of a pestilence model framework is difficult [10,11].

Many mathematical models have been constructed for COVID-19 without the vaccination and Quarantine compartment [12–15]. In this study, we combined the results of papers [16–20] to create an Omicron variant model with a variable population size.

The fractional derivatives have been utilized in the mathematical modeling of biological phenomena throughout the last few decades. This is due to the fact that fractional calculus can more precisely explain and process the retention and heritage characteristics of different materials than integer order models. As a result, many approaches have been used to examine the aforementioned field, including qualitative theory and numerical analysis. Therefore, using various mathematical methodologies, researchers enlarged the classical calculus to the fractional order. Considering mathematical models with fractional derivatives are effective instruments for researching infectious diseases [21–23]. The researchers looked at COVID-19 mathematical models using fractional order derivatives, and the findings were excellent [24–30].

We have constructed a fractional Omicron mathematical model in this research. The existence, uniqueness, and positivity of the solution are also deduced for the proposed Caputo-type fractional Omicron mathematical model by referring [31–35]. The paper is formulated as follows: In Sect. 2, we propose the fractional-order model by using Caputo fractional derivatives. In Sect. 3, we perform the qualitative analyses of the model containing the proofs of positivity and boundedness of the solution, existence of steady-state solutions, and the existence and uniqueness of the model solution. Computational simulations are done in Sect. 4 to validate and reinforce our theoretical findings for Omicron B.1.1.529 SARS-Cov-2. We conclude our findings in Sect. 5.

2 Model formulation

Firstly, we establish an integer-order model based on non-linear ordinary differential equations. The total population denoted by $N(t)$ is divided into state equations representing susceptible individuals $S(t)$, exposed individuals $E(t)$, infected individuals $I(t)$, quarantined individuals $Q(t)$, confirmed individuals $I_c(t)$, recovered individuals $R(t)$, vaccinated individuals $V(t)$, and the reservoir compartment $W(t)$.

In the model development, there are associated concerns that (i) the birth and death rates are specific. (ii) People who are susceptible get contaminated if they come into contact with an infectious person who is not vaccinated. (iii) Vaccines lose their effectiveness over time, causing people to lose their immunity. (iv) A person who has been infected recovers after therapy. (v) No long-term recovery is possible. (vi) The population has a homogeneous combination. (vii) For Omicron, the COVID-19 vaccinations are indicated. (viii) Vaccine can be given to isolated people. (ix) Individuals who have been separated may pass out as a result of their isolation.

In the model, we are going to use the following notations given in Table 1.

Considering the given aspects, the integer-order mathematical model is derived as follows:

$$\begin{aligned}
 \frac{dS}{dt} &= \Lambda - \delta_n S - \mu_s SI + \rho_r R + \rho_v V, \\
 \frac{dE}{dt} &= \mu_s SI - (\delta_n + k + \gamma_i + \delta_c)E, \\
 \frac{dI}{dt} &= \gamma_i E - (\delta_n + \delta_e + \nu_r + \tau + \omega_c)I, \\
 \frac{dQ}{dt} &= kE + \tau I + \zeta_q I_c - (\gamma_r + \eta_v + \delta_n)Q, \\
 \frac{dI_c}{dt} &= \delta_c E - (\zeta_q + \gamma_c + \zeta_w + \delta_n)I_c, \\
 \frac{dR}{dt} &= \nu_r I + \gamma_r Q + \gamma_c I_c - (\delta_n + \rho_r + \alpha_v)R, \\
 \frac{dV}{dt} &= \eta_v Q + \alpha_v R - (\delta_n + \rho_v)V, \\
 \frac{dW}{dt} &= \omega_c I + \zeta_w I_c - \delta_n W,
 \end{aligned} \tag{1}$$

with the initial conditions $S(0) = S_0, E(0) = E_0, I(0) = I_0, Q(0) = Q_0, I_c(0) = I_{c_0}, R(0) = R_0, V(0) = V_0, W(0) = W_0$.

2.1 Fractional-order model formulation

In the integer-order systems, the fading memory crossover effects and some others, like a random walk, cannot be captured. It means the classical systems do not contain memory because classical derivative operators are local and can-

Table 1 Parameters and their descriptions

Parameters	Descriptions
Λ	The rate of human recruitment into the community
μ_s	High seductive contact rate between the susceptible and sick people
α_v	The rate at which a given part of the recovering population is vaccinated
δ_n	The average death rate across all classes
ρ_r	The rate of losing medication immunity by recovered class
ρ_v	The value at which the immune system of the vaccinated compartment deteriorates
δ_e	The death rate caused by infected people’s contamination
δ_c	The rate at which exposed people progress from unconfirmed to confirmed class
ν_r	Because of several components, the regular recovery rates
τ	The diseased class’s treatment rate
ζ_q	Between confirmed and isolated people, there is a high rate of effective contact
η_v	Rate of getting vaccination of a specific part of isolated individuals
γ_c	The rate at which a particular subsection of confirmed people transitions to the recovered class
γ_i	The rate at which a particular subsection of exposed people becomes infected
γ_r	Contact rate between infected and recovered classes
ζ_w	Contact rate between the Confirmed people and reservoir
ω_c	Contact rate between the infected people and reservoir
k	Rate at which exposed people move to isolated class

not express the physical nature of the model efficiently. To overcome these drawbacks in our case, we consider a fractional-order model in this section.

Firstly, we recall the following definitions from fractional calculus.

Definition 1 Let Ψ be a continuous function on $[0, T]$. The Caputo fractional derivative is given by [36]

$${}^C D^\delta \Psi(t) = \frac{1}{\Gamma(n - \delta)} \int_0^t (t - \alpha)^{n-\delta-1} \frac{d^n}{d\alpha^n} \Psi(\alpha) d\alpha, \quad (2)$$

where $n = [\delta] + 1$ and $[\delta]$ represents the integer part function.

Definition 2 The Riemann–Liouville fractional integral is given by [36]

$$\mathcal{I}^\delta \Psi(t) = \frac{1}{\Gamma(\delta)} \int_0^t (t - \alpha)^{\delta-1} \Psi(\alpha) d\alpha. \quad (3)$$

We have mentioned that the classical models do not contain memory because memory effects can only be better captured by using fractional-order derivatives. Therefore, the corresponding model of fractional-order differential equations in the Caputo sense is written as follows:

$$\begin{aligned} {}^C D^\delta S &= \Lambda^\delta - \delta_n^\delta S - \mu_s^\delta SI + \rho_r^\delta R + \rho_v^\delta V, \\ {}^C D^\delta E &= \mu_s^\delta SI - (\xi_1)E, \\ {}^C D^\delta I &= \gamma_i^\delta E - (\xi_2)I, \\ {}^C D^\delta Q &= k^\delta E + \tau^\delta I + \zeta_q^\delta I_c - (\xi_3)Q, \end{aligned}$$

$$\begin{aligned} {}^C D^\delta I_c &= \delta_c^\delta E - (\xi_4)I_c, \\ {}^C D^\delta R &= \nu_r^\delta I + \gamma_r^\delta Q + \gamma_c^\delta I_c - (\xi_5)R, \\ {}^C D^\delta V &= \eta_v^\delta Q + \alpha_v^\delta R - (\xi_6)V, \\ {}^C D^\delta W &= \omega_c^\delta I + \zeta_w^\delta I_c - \delta_n^\delta W, \end{aligned} \quad (4)$$

where $\xi_1 = \delta_n^\delta + k^\delta + \gamma_i^\delta + \delta_c^\delta$, $\xi_2 = \delta_n^\delta + \delta_e^\delta + \nu_r^\delta + \tau^\delta + \omega_c^\delta$, $\xi_3 = \gamma_r^\delta + \eta_v^\delta + \delta_n^\delta$, $\xi_4 = \zeta_q^\delta + \gamma_c^\delta + \zeta_w^\delta + \delta_n^\delta$, $\xi_5 = \delta_n^\delta + \rho_r^\delta + \alpha_v^\delta$ and $\xi_6 = \delta_n^\delta + \rho_v^\delta$. The notation ${}^C D^\delta$ denotes the Caputo derivative operator with order δ . The model is defined subject to the initial conditions $S(0) = S_0, E(0) = E_0, I(0) = I_0, Q(0) = Q_0, I_c(0) = I_{c0}, R(0) = R_0, V(0) = V_0, W(0) = W_0$ (Fig. 1).

3 Qualitative analyses

Here we derive some important analyses to explore the characteristics of the proposed Caputo-type fractional order model.

3.1 Positivity and boundedness of the model

To check the non-negativity of the solution, we define $R_+^8 = \{\mathcal{U} \in R^8 \mid \mathcal{U} \geq 0\}$ and $\mathcal{U}(t) = (S(t), E(t), I(t), Q(t), I_c(t), R(t), V(t), W(t))^T$

We recall the generalized mean values theorem.

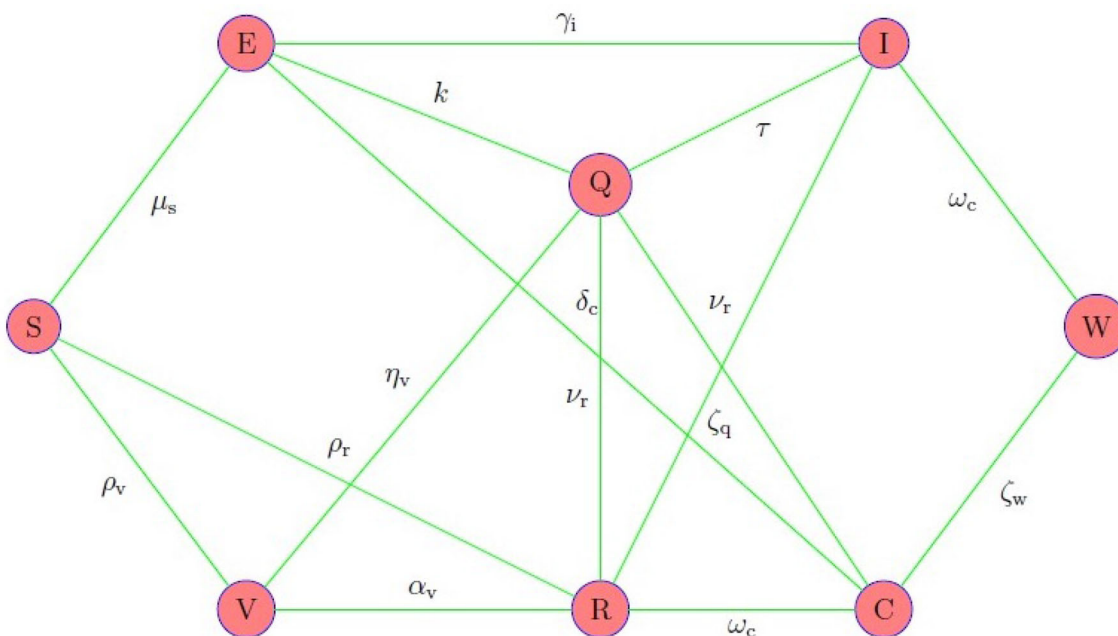


Fig. 1 Network of the model

Lemma 1 Let $U(t) \in C[a, b]$ and ${}^C D_t^\delta U(t) \in (a, b]$, then $U(t) = U(a) + \frac{1}{\Gamma(\delta)} ({}^C D_t^\delta U)(\zeta)(t - a)^\delta$ with $a \leq \zeta \leq t, \forall t \in (a, b]$.

Corollary 2 Let $U(t) \in C[a, b]$ and ${}^\delta D_t^C U(t) \in (a, b]$ where $\delta \in (0, 1]$. Then, it is clear from Lemma 1 that if ${}^\delta D_t^C U(t) \geq 0, \forall t \in (a, b]$, then the function $U(t)$ is non-decreasing, and if ${}^\delta D_t^C U(t) \leq 0, \forall t \in (a, b]$, then the function $U(t)$ is non-increasing for all $t \in [a, b]$.

To justify the non-negativity of the solution, it is necessary to show that the solution on every hyperplane bounding the positive orthant, the vector field points to R_+^8 .

Theorem 3 If $S(0), E(0), I(0), Q(0), I_c(0), R(0), V(0),$ and $W(0)$ are positive and bounded in R_+^8 , then $S(t), E(t), I(t), Q(t), I_c(t), R(t), V(t),$ and $W(t)$ are also positive and bounded in R_+^8 for all $t > 0$.

Proof From model (4), we get

$$\begin{aligned} {}^C D_t^\delta S(t)_{S=0} &= \rho_r^\delta R + \rho_v^\delta V \geq 0, \\ {}^C D_t^\delta E(t)_{E=0} &= \mu_s^\delta S I \geq 0, \\ {}^C D_t^\delta I(t)_{I=0} &= \gamma_i^\delta E \geq 0, \\ {}^C D_t^\delta Q(t)_{Q=0} &= k^\delta E + \tau^\delta I + \zeta_q^\delta I_c \geq 0, \\ {}^C D_t^\delta I_c(t)_{I_c=0} &= \delta_c^\delta E \geq 0, \\ {}^C D_t^\delta R(t)_{R=0} &= \nu_r^\delta I + \gamma_r^\delta Q + \gamma_c^\delta I_c \geq 0, \\ {}^C D_t^\delta V(t)_{V=0} &= \eta_v^\delta Q + \alpha_v^\delta R \geq 0, \\ {}^C D_t^\delta W(t)_{W=0} &= \omega_c^\delta I + \zeta_w^\delta I_c \geq 0, \end{aligned}$$

Therefore, applying Corollary 2, we get that our solution is nonnegative and will lie in the defined feasible region.

By adding the equations of the model (4), we get

$${}^C D_t^\delta N = \Lambda^\delta - (S + E + I + Q + I_c + R + V + W)\delta_n^\delta - \delta_e^\delta I, \tag{5}$$

which gives ${}^C D_t^\delta N \leq \Lambda^\delta - N\delta_n^\delta$. Thus, by taking Laplace transform we get

$$N(s) \leq \frac{\Lambda^\delta}{s(s^\delta + \delta_n^\delta)} + N(0) \frac{s^{(\delta-1)}}{s^\delta + \delta_n^\delta}. \tag{6}$$

By taking inverse Laplace transform and solving, we get

$$\lim_{t \rightarrow \infty} N(t) \leq \frac{\Lambda^\delta}{\delta_n^\delta}. \tag{7}$$

Then it follows the positivity and boundedness of (4) for all $t > 0$. □

3.2 Existence of steady state solutions

The model (4) is static, i.e., the time independent solutions exist. The steady state solution in the infection-free state, when $I = 0$, is derived by

$$\begin{aligned} E_q^0 &= (S^0, E^0, I^0, Q^0, I_c^0, R^0, V^0, W^0) \\ &= \left(\frac{\Lambda^\delta}{\delta_n^\delta}, 0, 0, 0, 0, 0, 0, 0 \right). \end{aligned} \tag{8}$$

In the presence of infection, i.e., $I \neq 0$, the steady state solution is derived by

$$E_q^1 = (S^1, E^1, I^1, Q^1, I_c^1, R^1, V^1, W^1), \tag{9}$$

where

$$\begin{aligned} S^1 &= \frac{\xi_2}{\gamma_i^\delta} \left(\frac{\Lambda^\delta \mu_s^\delta \gamma_i^\delta - \delta_n^\delta \xi_1 \xi_2}{\mu_s^\delta (\xi_1 \xi_2 - \rho_v^\delta \gamma_i^\delta J - \gamma_i^\delta G)} \right), \\ E^1 &= \frac{\xi_1 \xi_2}{\mu_s^\delta \gamma_i^\delta} \left(\frac{\Lambda^\delta \mu_s^\delta \gamma_i^\delta - \delta_n^\delta \xi_1 \xi_2}{\mu_s^\delta (\xi_1 \xi_2 - \rho_v^\delta \gamma_i^\delta J - \gamma_i^\delta G)} \right), \\ I^1 &= \frac{\Lambda^\delta \mu_s^\delta \gamma_i^\delta - \delta_n^\delta \xi_1 \xi_2}{\mu_s^\delta (\xi_1 \xi_2 - \rho_v^\delta \gamma_i^\delta J - \gamma_i^\delta G)}, \\ Q^1 &= \frac{\xi_2 \xi_4 + \tau^\delta \xi_4 \gamma_i^\delta + \zeta_q^\delta \delta_c^\delta \xi_2}{\xi_3 \xi_4 \gamma_i^\delta} \left(\frac{\Lambda^\delta \mu_s^\delta \gamma_i^\delta - \delta_n^\delta \xi_1 \xi_2}{\mu_s^\delta (\xi_1 \xi_2 - \rho_v^\delta \gamma_i^\delta J - \gamma_i^\delta G)} \right), \\ I_c^1 &= \frac{\delta_c^\delta \xi_2}{\xi_4 \gamma_i^\delta} \left(\frac{\Lambda^\delta \mu_s^\delta \gamma_i^\delta - \delta_n^\delta \xi_1 \xi_2}{\mu_s^\delta (\xi_1 \xi_2 - \rho_v^\delta \gamma_i^\delta J - \gamma_i^\delta G)} \right), \\ R^1 &= \frac{\nu_r^\delta \gamma_i^\delta \xi_3 \xi_4 + \gamma_r^\delta (\xi_2 \xi_4 + \tau^\delta \xi_4 \gamma_i^\delta + \zeta_q^\delta \delta_c^\delta \xi_2) + \gamma_i^\delta \delta_c^\delta \xi_2 \xi_3}{\gamma_i^\delta \xi_3 \xi_4 \xi_5} \\ &\quad \left(\frac{\Lambda^\delta \mu_s^\delta \gamma_i^\delta - \delta_n^\delta \xi_1 \xi_2}{\mu_s^\delta (\xi_1 \xi_2 - \rho_v^\delta \gamma_i^\delta J - \gamma_i^\delta G)} \right), \\ V^1 &= \frac{\eta_v^\delta \gamma_i^\delta \xi_5 (\xi_2 \xi_4 + \tau^\delta \xi_4 \gamma_i^\delta + \zeta_q^\delta \delta_c^\delta \xi_2)}{\xi_3 \xi_4 \gamma_i^\delta \xi_5} \\ &\quad + \frac{\alpha_v^\delta [\nu_r^\delta \gamma_i^\delta \xi_3 \xi_4 + \gamma_r^\delta (\xi_2 \xi_4 + \tau^\delta \xi_4 \gamma_i^\delta + \zeta_q^\delta \delta_c^\delta \xi_2) + \gamma_i^\delta \delta_c^\delta \xi_2 \xi_3]}{\xi_3 \xi_4 \gamma_i^\delta \xi_5} \\ &\quad \left(\frac{\Lambda^\delta \mu_s^\delta \gamma_i^\delta - \delta_n^\delta \xi_1 \xi_2}{\mu_s^\delta (\xi_1 \xi_2 - \rho_v^\delta \gamma_i^\delta J - \gamma_i^\delta G)} \right), \\ W^1 &= \frac{\gamma_i^\delta \omega_c^\delta \xi_4 + \zeta_w^\delta \delta_c^\delta \xi_2}{\delta_n^\delta \gamma_i^\delta \xi_4} \left(\frac{\Lambda^\delta \mu_s^\delta \gamma_i^\delta - \delta_n^\delta \xi_1 \xi_2}{\mu_s^\delta (\xi_1 \xi_2 - \rho_v^\delta \gamma_i^\delta J - \gamma_i^\delta G)} \right), \end{aligned}$$

with

$$\begin{aligned} J &= \frac{\nu_r^\delta \gamma_i^\delta \xi_3 \xi_4 + \gamma_r^\delta (\xi_2 \xi_4 + \tau^\delta \xi_4 \gamma_i^\delta + \zeta_q^\delta \delta_c^\delta \xi_2) + \gamma_i^\delta \delta_c^\delta \xi_2 \xi_3}{\gamma_i^\delta \xi_3 \xi_4 \xi_5}, \\ G &= \frac{\eta_v^\delta \gamma_i^\delta \xi_5 (\xi_2 \xi_4 + \tau^\delta \xi_4 \gamma_i^\delta + \zeta_q^\delta \delta_c^\delta \xi_2)}{\xi_3 \xi_4 \gamma_i^\delta \xi_5} \\ &\quad + \frac{\alpha_v^\delta [\nu_r^\delta \gamma_i^\delta \xi_3 \xi_4 + \gamma_r^\delta (\xi_2 \xi_4 + \tau^\delta \xi_4 \gamma_i^\delta + \zeta_q^\delta \delta_c^\delta \xi_2) + \gamma_i^\delta \delta_c^\delta \xi_2 \xi_3]}{\xi_3 \xi_4 \gamma_i^\delta \xi_5}. \end{aligned}$$

The fundamental reproduction number R_0 is calculated by next generation matrix method [37,38]. Hence, R_0 is given by

$$\begin{aligned} R_0(GV^{-1}) &= \frac{\Lambda^\delta \mu_s^\delta \gamma_i^\delta}{\delta_n^\delta (\delta_n^\delta + k^\delta + \gamma_i^\delta + \delta_c^\delta) (\delta_n^\delta + \delta_e^\delta + \nu_r^\delta + \tau^\delta + \omega_c^\delta)}. \tag{10} \end{aligned}$$

When $R_0 < 1$, contaminations are disappearing from the host population. However, if $R_0 > 1$, the contaminations harm and become endemic, likely to require appropriate clinical treatments to halt the disease's spread.

Theorem 4 *The disease-free equilibrium E_0 of the proposed model (4) is stable if $R_0 < 1$ and unstable if $R_0 > 1$.*

Proof To derive the stability analysis of the disease-free equilibrium points, we consider the linearization of the given model at any equilibrium point $(S^0, E^0, I^0, Q^0, I_c^0, R^0, V^0, W^0)$ as follows:

$$\begin{aligned} {}^C D^\delta S &= \Lambda^\delta - \delta_n^\delta S - \mu_s^\delta S^* I - \mu_s^\delta S I^* + \rho_r^\delta R + \rho_v^\delta V, \\ {}^C D^\delta E &= \mu_s^\delta S^* I + \mu_s^\delta S I^* - (\xi_1) E, \\ {}^C D^\delta I &= \gamma_i^\delta E - (\xi_2) I, \\ {}^C D^\delta Q &= k^\delta E + \tau^\delta I + \zeta_q^\delta I_c - (\xi_3) Q, \\ {}^C D^\delta I_c &= \delta_c^\delta E - (\xi_4) I_c, \\ {}^C D^\delta R &= \nu_r^\delta I + \gamma_r^\delta Q + \gamma_c^\delta I_c - (\xi_5) R, \\ {}^C D^\delta V &= \eta_v^\delta Q + \alpha_v^\delta R - (\xi_6) V, \\ {}^C D^\delta W &= \omega_c^\delta I + \zeta_w^\delta I_c - \delta_n^\delta W. \end{aligned} \tag{11}$$

Using the Laplace transformation on both sides of above system provides

$$\begin{aligned} s^\delta \mathcal{L}[S(s)] - s^{\delta-1} S(0) &= \Lambda^\delta - \delta_n^\delta \mathcal{L}[S(s)] - \mu_s^\delta I^* \mathcal{L}[S(s)] - \mu_s^\delta S^* \mathcal{L}[I(s)] \\ &\quad + \rho_r^\delta \mathcal{L}[R(s)] + \rho_v^\delta \mathcal{L}[V(s)], \\ s^\delta \mathcal{L}[E(s)] - s^{\delta-1} E(0) &= \mu_s^\delta I^* \mathcal{L}[S(s)] + \mu_s^\delta S^* \mathcal{L}[I(s)] - (\xi_1) \mathcal{L}[E(s)], \\ s^\delta \mathcal{L}[I(s)] - s^{\delta-1} I(0) &= \gamma_i^\delta \mathcal{L}[E(s)] - (\xi_2) \mathcal{L}[I(s)], \\ s^\delta \mathcal{L}[Q(s)] - s^{\delta-1} Q(0) &= k^\delta \mathcal{L}[E(s)] + \tau^\delta \mathcal{L}[I(s)] + \zeta_q^\delta \mathcal{L}[I_c(s)] - (\xi_3) \mathcal{L}[Q(s)], \\ s^\delta \mathcal{L}[I_c(s)] - s^{\delta-1} I_c(0) &= \delta_c^\delta \mathcal{L}[E(s)] - (\xi_4) \mathcal{L}[I_c(s)], \\ s^\delta \mathcal{L}[R(s)] - s^{\delta-1} R(0) &= \nu_r^\delta \mathcal{L}[I(s)] + \gamma_r^\delta \mathcal{L}[Q(s)] + \gamma_c^\delta \mathcal{L}[I_c(s)] - (\xi_5) \mathcal{L}[R(s)], \\ s^\delta \mathcal{L}[V(s)] - s^{\delta-1} V(0) &= \eta_v^\delta \mathcal{L}[Q(s)] + \alpha_v^\delta \mathcal{L}[R(s)] - (\xi_6) \mathcal{L}[V(s)], \\ s^\delta \mathcal{L}[W(s)] - s^{\delta-1} W(0) &= \omega_c^\delta \mathcal{L}[I(s)] + \zeta_w^\delta \mathcal{L}[I_c(s)] - \delta_n^\delta \mathcal{L}[W(s)], \end{aligned} \tag{12}$$

where $\mathcal{L}[S(s)], \mathcal{L}[E(s)], \mathcal{L}[I(s)], \mathcal{L}[Q(s)], \mathcal{L}[I_c(s)], \mathcal{L}[R(s)], \mathcal{L}[V(s)],$ and $\mathcal{L}[W(s)]$ are the Laplace transformations of $S(t), E(t), I(t), Q(t), I_c(t), R(t), V(t),$ and $W(t)$. The proposed system (12) can be rewritten by

$$\begin{aligned} \Delta(s) \cdot [L[S(s)]L[E(s)]L[I(s)]L[Q(s)] \\ [L[I_c(s)]L[R(s)]L[V(s)]L[W(s)]] \\ = [\nu_1(s)\nu_2(s)\nu_3(s)\nu_4(s)\nu_5(s)\nu_6(s)\nu_7(s)\nu_8(s)], \end{aligned}$$

where

$$\begin{cases} v_1(s) = s^{\delta-1}S(0), \\ v_2(s) = s^{\delta-1}E(0), \\ v_3(s) = s^{\delta-1}I(0), \\ v_4(s) = s^{\delta-1}Q(0), \\ v_5(s) = s^{\delta-1}I_c(0), \\ v_6(s) = s^{\delta-1}R(0), \\ v_7(s) = s^{\delta-1}V(0), \\ v_8(s) = s^{\delta-1}W(0), \end{cases}$$

To find the existence of solution, a Banach space is defined as $\mathcal{B} = B_1 \times B_2 \times B_3 \times B_4 \times B_5 \times B_6 \times B_7 \times B_8$, where $B_i = C([0, T])$, ($i = 1, 2, \dots, 8$) under the norm $\|\mathcal{U}\| = \|(S, E, I, Q, I_c, R, V, W)\| = \max_{t \in [0, T]} [|S(t)|, |E(t)|, |I(t)|, |Q(t)|, |I_c(t)|, |R(t)|, |V(t)|, |W(t)|]$.

Let $\mathcal{Z} : A \rightarrow A$ be an operator defined as follows:

$$\Delta(s) = \begin{bmatrix} s^\delta + \delta_n^\delta + \mu_s^\delta I^* & 0 & \mu_s^\delta S^* & 0 & 0 & -\rho_r^\delta & -\rho_v^\delta & 0 \\ -\mu_s^\delta I^* & s^\delta + \xi_1 & -\mu_s^\delta S^* & 0 & 0 & 0 & 0 & 0 \\ 0 & -\gamma_i^\delta & s^\delta + \xi_2 & 0 & 0 & 0 & 0 & 0 \\ 0 & -k & -\tau^\delta & s^\delta + \xi_3 & -\zeta_q^\delta & 0 & 0 & 0 \\ 0 & -\delta_c^\delta & 0 & 0 & s^\delta + \xi_4 & 0 & 0 & 0 \\ 0 & 0 & -\nu_r^\delta & -\gamma_r^\delta & -\gamma_c^\delta & s^\delta + \xi_5 & 0 & 0 \\ 0 & 0 & 0 & -\eta_v^\delta & 0 & -\alpha_v^\delta & s^\delta + \xi_6 & 0 \\ 0 & 0 & -\omega_c^\delta & 0 & -\zeta_w^\delta & 0 & 0 & s^\delta + \delta_n^\delta \end{bmatrix},$$

which is a characteristic matrix of system (12). Now, the characteristic matrix of the given system at disease-free equilibrium (DFE) $E_q^0 = (\frac{\Lambda^\delta}{\delta_n^\delta}, 0, 0, 0, 0, 0, 0, 0)$ is given by

$$\Delta(s) = \begin{bmatrix} s^\delta + \delta_n^\delta & 0 & \mu_s^\delta S^* & 0 & 0 & -\rho_r^\delta & -\rho_v^\delta & 0 \\ 0 & s^\delta + \xi_1 & -\mu_s^\delta S^* & 0 & 0 & 0 & 0 & 0 \\ 0 & -\gamma_i^\delta & s^\delta + \xi_2 & 0 & 0 & 0 & 0 & 0 \\ 0 & -k & -\tau^\delta & s^\delta + \xi_3 & -\zeta_q^\delta & 0 & 0 & 0 \\ 0 & -\delta_c^\delta & 0 & 0 & s^\delta + \xi_4 & 0 & 0 & 0 \\ 0 & 0 & -\nu_r^\delta & -\gamma_r^\delta & -\gamma_c^\delta & s^\delta + \xi_5 & 0 & 0 \\ 0 & 0 & 0 & -\eta_v^\delta & 0 & -\alpha_v^\delta & s^\delta + \xi_6 & 0 \\ 0 & 0 & -\omega_c^\delta & 0 & -\zeta_w^\delta & 0 & 0 & s^\delta + \delta_n^\delta \end{bmatrix}.$$

The eigenvalues are $-\delta_n^\delta, -\delta_n^\delta, \frac{1}{2}(-\xi_1 - \xi_2 - \sqrt{\xi_1^2 + 4\mu_s^\delta S^* \gamma_i^\delta - 2\xi_1 \xi_2 + \xi_2^2}), \frac{1}{2}(-\xi_1 - \xi_2 + \sqrt{\xi_1^2 + 4\mu_s^\delta S^* \gamma_i^\delta - 2\xi_1 \xi_2 + \xi_2^2}), -\xi_3, -\xi_4, -\xi_5, -\xi_6$. The given system (4) is stable when $-\xi_1 - \xi_2 + \sqrt{\xi_1^2 + 4\mu_s^\delta S^* \gamma_i^\delta - 2\xi_1 \xi_2 + \xi_2^2} < 0$ or $\sqrt{\xi_1^2 + 4\mu_s^\delta S^* \gamma_i^\delta - 2\xi_1 \xi_2 + \xi_2^2} < (\xi_1 + \xi_2)$ or $\xi_1^2 + 4\mu_s^\delta S^* \gamma_i^\delta - 2\xi_1 \xi_2 + \xi_2^2 < (\xi_1 + \xi_2)^2$ or $\mu_s^\delta S^* \gamma_i^\delta < \xi_1 \xi_2$, i.e., $\frac{\mu_s^\delta S^* \gamma_i^\delta}{\xi_1 \xi_2} < 1$. That is $R_0 < 1$. Clearly, infection free steady state E^0 is locally asymptotically stable if $R_0 < 1$ and unstable if $R_0 > 1$. \square

3.3 Existence and uniqueness

The system (4) can be written in the form:

$$\begin{aligned} {}^C D^\delta U(t) &= \mathcal{H}(t, \mathcal{U}(t)), \quad 0 < \delta \leq 1, \\ U(0) &= U_0. \end{aligned} \tag{13}$$

$$\mathcal{Z}(\mathcal{U})(t) = Z_0 + \frac{1}{\Gamma(\delta)} \int_0^t (t - \alpha)^{\delta-1} \mathcal{H}(\alpha, \mathcal{U}(\alpha)) d\alpha.$$

Using the Riemann Liouville type integral, Eq. (13) solved as follows: $\mathcal{U}(t) = \mathcal{U}_0 + \frac{1}{\Gamma(\delta)} \int_0^t (t - \alpha)^{\delta-1} \mathcal{H}(\alpha, \mathcal{U}(\alpha)) d\alpha$ where

$$\begin{cases} S(t) = S_0 + \frac{1}{\Gamma(\delta)} \int_0^t (t - \alpha)^{\delta-1} \mathcal{H}(\alpha, S) d\alpha, \\ E(t) = E_0 + \frac{1}{\Gamma(\delta)} \int_0^t (t - \alpha)^{\delta-1} \mathcal{H}(\alpha, E) d\alpha, \\ I(t) = I_0 + \frac{1}{\Gamma(\delta)} \int_0^t (t - \alpha)^{\delta-1} \mathcal{H}(\alpha, I) d\alpha, \\ Q(t) = Q_0 + \frac{1}{\Gamma(\delta)} \int_0^t (t - \alpha)^{\delta-1} \mathcal{H}(\alpha, Q) d\alpha, \\ I_c(t) = I - c_0 + \frac{1}{\Gamma(\delta)} \int_0^t (t - \alpha)^{\delta-1} \mathcal{H}(\alpha, I_c) d\alpha, \\ R(t) = R_0 + \frac{1}{\Gamma(\delta)} \int_0^t (t - \alpha)^{\delta-1} \mathcal{H}(\alpha, R) d\alpha, \\ V(t) = V_0 + \frac{1}{\Gamma(\delta)} \int_0^t (t - \alpha)^{\delta-1} \mathcal{H}(\alpha, V) d\alpha, \\ W(t) = W_0 + \frac{1}{\Gamma(\delta)} \int_0^t (t - \alpha)^{\delta-1} \mathcal{H}(\alpha, W) d\alpha, \end{cases} \tag{14}$$

with

$$\begin{cases} \mathcal{H}(t, S) = \Lambda^\delta - \delta_n^\delta S - \mu_s^\delta SI + \rho_r^\delta R + \rho_v^\delta V, \\ \mathcal{H}(t, E) = \mu_s^\delta SI - (\xi_1)E, \\ \mathcal{H}(t, I) = \gamma_i^\delta E - (\xi_2)I, \\ \mathcal{H}(t, Q) = k^\delta E + \tau^\delta I + \zeta_q^\delta I_c - (\xi_3)Q, \\ \mathcal{H}(t, I_c) = \delta_c^\delta E - (\xi_4)I_c, \\ \mathcal{H}(t, R) = \nu_r^\delta I + \gamma_r^\delta Q + \gamma_c^\delta I_c - (\xi_5)R, \\ \mathcal{H}(t, V) = \eta_v^\delta Q + \alpha_v^\delta R - (\xi_6)V, \\ \mathcal{H}(t, W) = \omega_c^\delta I + \zeta_w^\delta I_c - \delta_n^\delta W. \end{cases} \tag{15}$$

The following theorems show the existence of a solution.

Theorem 5 *Let $S(t), E(t), I(t), Q(t), I_c(t), R(t), V(t)$ and $W(t)$ be nonnegative bounded functions. Then the system (15) satisfies Lipschitz condition are contraction mappings, if the following condition holds, $0 \leq N = \max\{\mathcal{F}_{\mathcal{H}_1}, \mathcal{F}_{\mathcal{H}_2}, \mathcal{F}_{\mathcal{H}_3}, \mathcal{F}_{\mathcal{H}_4}, \mathcal{F}_{\mathcal{H}_5}, \mathcal{F}_{\mathcal{H}_6}, \mathcal{F}_{\mathcal{H}_7}, \mathcal{F}_{\mathcal{H}_8}\} < 1$, the functions are contractions.*

Proof Assume that $S(t), E(t), I(t), Q(t), I_c(t), R(t), V(t)$ and $W(t)$ are nonnegative bounded functions. That is, there are some positive constants $\beta_1, \beta_2, \beta_3, \beta_4, \beta_5, \beta_6, \beta_7, \beta_8$, such that $\|S(t)\| \leq \beta_1, \|E(t)\| \leq \beta_2, \|I(t)\| \leq \beta_3, \|Q(t)\| \leq \beta_4, \|I_c(t)\| \leq \beta_5, \|R(t)\| \leq \beta_6, \|V(t)\| \leq \beta_7, \|W(t)\| \leq \beta_8$.

Considering the function $\mathcal{H}(\alpha, S)$, for any S and S_1 , we can get

$$\begin{aligned} \|\mathcal{H}(\alpha, S) - \mathcal{H}(\alpha, S_1)\| &= \|\delta_n^\delta (S - S_1) + \mu_s^\delta I (S - S_1)\| \\ &\leq \|\delta_n^\delta (S - S_1)\| + \|\mu_s^\delta I (S - S_1)\| \\ &\leq (\delta_n^\delta + \mu_s^\delta \|I(t)\|) \|S - S_1\| \\ &\leq (\delta_n^\delta + \mu_s^\delta \beta_3) \|S - S_1\| \\ &\leq \mathcal{F}_{\mathcal{H}_1} \|S - S_1\|. \end{aligned} \tag{16}$$

where $\mathcal{F}_{\mathcal{H}_1} = \delta_n^\delta + \mu_s^\delta \beta_3$. Hence, $\mathcal{H}(\alpha, S)$ satisfies the Lipschitz condition. Similarly, we can find $\mathcal{F}_{\mathcal{H}_i}$, for $i = 2, 3, 4, 5, 6, 7, 8$ so that $\mathcal{H}(\alpha, S), \mathcal{H}(\alpha, E), \mathcal{H}(\alpha, I), \mathcal{H}(\alpha, Q), \mathcal{H}(\alpha, I_c), \mathcal{H}(\alpha, R), \mathcal{H}(\alpha, V)$, and $\mathcal{H}(\alpha, W)$ satisfy the Lipschitz's conditions.

Also, when the condition $0 \leq N = \max\{\mathcal{F}_{\mathcal{H}_1}, \mathcal{F}_{\mathcal{H}_2}, \mathcal{F}_{\mathcal{H}_3}, \mathcal{F}_{\mathcal{H}_4}, \mathcal{F}_{\mathcal{H}_5}, \mathcal{F}_{\mathcal{H}_6}, \mathcal{F}_{\mathcal{H}_7}, \mathcal{F}_{\mathcal{H}_8}\} < 1$ holds, the functions are contractions. \square

Equation (14) can be formulated as follows:

$$U_n(t) = \begin{cases} S_n(t) = S_0 + \frac{1}{\Gamma(\delta)} \int_0^t (t - \alpha)^{\delta-1} \mathcal{H}(\alpha, S_{n-1}) d\alpha, \\ E_n(t) = E_0 + \frac{1}{\Gamma(\delta)} \int_0^t (t - \alpha)^{\delta-1} \mathcal{H}(\alpha, E_{n-1}) d\alpha, \\ I_n(t) = I_0 + \frac{1}{\Gamma(\delta)} \int_0^t (t - \alpha)^{\delta-1} \mathcal{H}(\alpha, I_{n-1}) d\alpha, \\ Q_n(t) = Q_0 + \frac{1}{\Gamma(\delta)} \int_0^t (t - \alpha)^{\delta-1} \mathcal{H}(\alpha, Q_{n-1}) d\alpha, \\ I_{c_n}(t) = I - c_0 + \frac{1}{\Gamma(\delta)} \int_0^t (t - \alpha)^{\delta-1} \mathcal{H}(\alpha, I_{c_{n-1}}) d\alpha, \\ R_n(t) = R_0 + \frac{1}{\Gamma(\delta)} \int_0^t (t - \alpha)^{\delta-1} \mathcal{H}(\alpha, R_{n-1}) d\alpha, \\ V_n(t) = V_0 + \frac{1}{\Gamma(\delta)} \int_0^t (t - \alpha)^{\delta-1} \mathcal{H}(\alpha, V_{n-1}) d\alpha, \\ W_n(t) = W_0 + \frac{1}{\Gamma(\delta)} \int_0^t (t - \alpha)^{\delta-1} \mathcal{H}(\alpha, W_{n-1}) d\alpha. \end{cases}$$

The provided initial conditions establish the first elements of the given equations. The contrast between two terms is expressed by

$$\begin{aligned} \Psi_{1_n}(t) &= S_n(t) - S_{n-1}(t) \\ &= \frac{1}{\Gamma(\delta)} \int_0^t [\mathcal{H}(\alpha, S_{n-1}) - \mathcal{H}(\alpha, S_{n-2})] d\alpha, \\ \Psi_{2_n}(t) &= E_n(t) - E_{n-1}(t) \\ &= \frac{1}{\Gamma(\delta)} \int_0^t [\mathcal{H}(\alpha, E_{n-1}) - \mathcal{H}(\alpha, E_{n-2})] d\alpha, \\ \Psi_{3_n}(t) &= I_n(t) - I_{n-1}(t) \\ &= \frac{1}{\Gamma(\delta)} \int_0^t [\mathcal{H}(\alpha, S_{n-1}) - \mathcal{H}(\alpha, S_{n-2})] d\alpha, \\ \Psi_{4_n}(t) &= Q_n(t) - Q_{n-1}(t) \\ &= \frac{1}{\Gamma(\delta)} \int_0^t [\mathcal{H}(\alpha, Q_{n-1}) - \mathcal{H}(\alpha, Q_{n-2})] d\alpha, \\ \Psi_{5_n}(t) &= I_{c_n}(t) - I_{c_{n-1}}(t) \\ &= \frac{1}{\Gamma(\delta)} \int_0^t [\mathcal{H}(\alpha, I_{c_{n-1}}) - \mathcal{H}(\alpha, I_{c_{n-2}})] d\alpha, \\ \Psi_{6_n}(t) &= R_n(t) - R_{n-1}(t) \\ &= \frac{1}{\Gamma(\delta)} \int_0^t [\mathcal{H}(\alpha, R_{n-1}) - \mathcal{H}(\alpha, R_{n-2})] d\alpha, \\ \Psi_{7_n}(t) &= V_n(t) - V_{n-1}(t) \\ &= \frac{1}{\Gamma(\delta)} \int_0^t [\mathcal{H}(\alpha, V_{n-1}) - \mathcal{H}(\alpha, V_{n-2})] d\alpha, \\ \Psi_{8_n}(t) &= W_n(t) - W_{n-1}(t) \\ &= \frac{1}{\Gamma(\delta)} \int_0^t [\mathcal{H}(\alpha, W_{n-1}) - \mathcal{H}(\alpha, W_{n-2})] d\alpha, \end{aligned}$$

where

$$U_n(t) = \begin{cases} S_n(t) = \sum_{i=0}^n \Psi_{1_i}(t), & E_n(t) = \sum_{i=0}^n \Psi_{2_i}(t), \\ I_n(t) = \sum_{i=0}^n \Psi_{3_i}(t), & Q_n(t) = \sum_{i=0}^n \Psi_{4_i}(t), \\ I_{c_n}(t) = \sum_{i=0}^n \Psi_{5_i}(t), & R_n(t) = \sum_{i=0}^n \Psi_{6_i}(t), \\ V_n(t) = \sum_{i=0}^n \Psi_{7_i}(t), & W_n(t) = \sum_{i=0}^n \Psi_{8_i}(t). \end{cases} \tag{17}$$

Consider

$$\begin{aligned} \|\Psi_{1_n}(t)\| &= \|S_n(t) - S_{n-1}(t)\| \\ &= \frac{1}{\Gamma(\delta)} \int_0^t [\mathcal{H}(\alpha, S_{n-1}) - \mathcal{H}(\alpha, S_{n-1})] d\alpha \\ &= \frac{\beta_1}{\Gamma(\delta)} \int_0^t \|S_{n-1} - S_{n-2}\| d\alpha \\ &= \frac{\beta_1}{\Gamma(\delta)} \int_0^t \|\Psi_{1_{n-1}}(t)\| d\alpha. \end{aligned}$$

Hence, we can get

$$\|\Psi_{i_n}(t)\| = \frac{\beta_i}{\Gamma(\delta)} \int_0^t \|\Psi_{i_{n-1}}(t)\| d\alpha \text{ for } i = 1, 2, \dots, 8. \tag{18}$$

The system (17) exists and smooth.

For, we have that the functions $S(t), E(t), I(t), Q(t), I_c(t), R(t), V(t)$ and $W(t)$ are bounded and all kernels $\mathcal{H}(t, S), \mathcal{H}(t, E), \mathcal{H}(t, I), \mathcal{H}(t, Q), \mathcal{H}(t, I_c), \mathcal{H}(t, R), \mathcal{H}(t, V)$ and $\mathcal{H}(t, W)$ fulfill Lipschitz's conditions; thus, we get the following relations:

$$\begin{cases} \|\Psi_{1_n}(t)\| \leq \|S(0)\| \left\| \frac{\beta_1}{\Gamma(\delta)} t \right\|^n, & \|\Psi_{2_n}(t)\| \leq \|E(0)\| \left\| \frac{\beta_2}{\Gamma(\delta)} t \right\|^n, \\ \|\Psi_{3_n}(t)\| \leq \|I(0)\| \left\| \frac{\beta_3}{\Gamma(\delta)} t \right\|^n, & \|\Psi_{4_n}(t)\| \leq \|Q(0)\| \left\| \frac{\beta_4}{\Gamma(\delta)} t \right\|^n, \\ \|\Psi_{5_n}(t)\| \leq \|I_c(0)\| \left\| \frac{\beta_5}{\Gamma(\delta)} t \right\|^n, & \|\Psi_{6_n}(t)\| \leq \|R(0)\| \left\| \frac{\beta_6}{\Gamma(\delta)} t \right\|^n, \\ \|\Psi_{7_n}(t)\| \leq \|V(0)\| \left\| \frac{\beta_7}{\Gamma(\delta)} t \right\|^n, & \|\Psi_{8_n}(t)\| \leq \|W(0)\| \left\| \frac{\beta_8}{\Gamma(\delta)} t \right\|^n. \end{cases} \tag{19}$$

The system (19) shows the existence and smoothness of the function defined in (17).

Theorem 6 Let $\mathcal{Z} : \mathcal{A} \rightarrow \mathcal{A}$ be completely continuous and let $\mathcal{H} : [0, T] \times \mathcal{A} \rightarrow \mathbb{R}$ be continuous and there exists a constant $\mathcal{F}_{\mathcal{H}} > 0$ such that for $U, U_1 \in \mathcal{A}$,

$$|\mathcal{H}(t, U) - \mathcal{H}(t, U_1)| \leq \mathcal{F}_{\mathcal{H}}|U - U_1|$$

is hold. Then there is at least one solution for the considered system (4).

Proof To prove the operator, \mathcal{Z} is completely continuous. The sequence $\{U_n\}$ converges to $U \in \mathcal{A}$. After n-iterations define the remainder terms as $D_{1_n}(t), D_{2_n}(t), D_{3_n}(t), D_{4_n}(t), D_{5_n}(t), D_{6_n}(t), D_{7_n}(t), D_{8_n}(t)$, such that

$$\begin{aligned} S(t) - S(0) &= S_n(t) - D_{1_n}(t), & E(t) - E(0) &= E_n(t) - D_{2_n}(t) \\ I(t) - I(0) &= I_n(t) - D_{3_n}(t), & Q(t) - Q(0) &= Q_n(t) - D_{4_n}(t), \\ I_c(t) - I_c(0) &= I_{c_n}(t) - D_{5_n}(t), & R(t) - R(0) &= R_n(t) - D_{6_n}(t), \\ V(t) - V(0) &= V_n(t) - D_{7_n}(t), & W(t) - W(0) &= W_n(t) - D_{8_n}(t). \end{aligned}$$

Using triangle inequality along with the Lipschitz condition of $\mathcal{H}(t, S)$, we obtain:

$$\begin{aligned} \|D_{1_n}(t)\| &= \frac{1}{\Gamma(\delta)} \int_0^t [\mathcal{H}(\alpha, S) - \mathcal{H}(\alpha, S_{n-1})] d\alpha \\ &\leq \frac{\beta_1}{\Gamma(\delta)} \|S - S_{n-1}\| t. \end{aligned}$$

Using the above process recursively, we get

$$\|D_{1_n}(t)\| \leq \left\| \frac{C_1}{\Gamma(\delta)} t \right\|^{n+1} \beta_1.$$

Then, at $t_0 > 1$

$$\|D_n(t)\| \leq \left\| \frac{C_1}{\Gamma(\delta)} t_0 \right\|^{n+1} \beta_1.$$

Taking limit as n tends to infinity, we get

$$\lim_{n \rightarrow \infty} \|D_{1_n}(t)\| \leq \lim_{n \rightarrow \infty} \left\| \frac{C_1}{\Gamma(\delta)} t_0 \right\|^{n+1} \beta_1. \tag{20}$$

For $\frac{C_1}{\Gamma(\delta)} t_0 < 1$, Eq. (20) becomes $\lim_{n \rightarrow \infty} \|D_{1_n}(t)\| = 0$. Similarly, as n tends to infinity, we can get $\|D_{i_n}(t)\| \rightarrow 0$.

Hence, for $t \in [0, T]$, we have $S_n(t) \rightarrow S(t)$ as $n \rightarrow \infty$, and therefore,

$$\begin{aligned} \|\mathcal{Z}(S_n) - \mathcal{Z}(S)\| &\leq \frac{1}{\Gamma(\delta)} \max_{t \in [0, T]} \int_0^t (t - \alpha)^{\delta-1} |\mathcal{H}(\alpha, S_n(\alpha)) - \mathcal{H}(\alpha, S(\alpha))| d\alpha, \\ &\leq \frac{\mathcal{F}_{\mathcal{H}}}{\Gamma(\delta)} \|S_n - S\|_{t \in [0, T]} \\ &\int_0^t (t - \alpha)^{\delta-1} d\alpha \leq \frac{T^\delta \mathcal{F}_{\mathcal{H}}}{\Gamma(\delta + 1)} \|S_n - S\|. \end{aligned}$$

Since $S_n \rightarrow S, \|\mathcal{Z}(S_n) - \mathcal{Z}(S)\| \rightarrow 0$ as $n \rightarrow \infty$ and hence $\|\mathcal{Z}(U_n) - \mathcal{Z}(U)\| \rightarrow 0$ as $n \rightarrow \infty$. Thus, \mathcal{Z} is continuous. Let a bounded set $\mathcal{M} \subset \mathcal{A}$. Then by definition of $\mathcal{A}, |\mathcal{H}(t, \mathcal{U}(t))| \leq \mathcal{L}_{\mathcal{H}}, \mathcal{L}_{\mathcal{H}} > 0, \forall U \in \mathcal{M}$. Then for each $U \in \mathcal{M}$, we can obtain

$$\begin{aligned} \|\mathcal{Z}(U)\| &\leq \frac{1}{\Gamma(\delta)} \max_{t \in [0, T]} \int_0^t (t - \alpha)^{\delta-1} |\mathcal{H}(\alpha, Z(\alpha))| d\alpha \\ &\leq \frac{\mathcal{L}_{\mathcal{H}}}{\Gamma(\delta)} \max_{t \in [0, T]} \int_0^t (t - \alpha)^{\delta-1} d\alpha \leq \frac{T^\delta \mathcal{L}_{\mathcal{H}}}{\Gamma(\delta + 1)}. \end{aligned}$$

Thus, \mathcal{Z} is uniformly bounded. Further, suppose $0 \leq t_2 \leq t_1 \leq T$. Then

$$\begin{aligned} \|\mathcal{Z}(U)(t_1) - \mathcal{Z}(U)(t_2)\| &\leq \frac{\mathcal{L}_{\mathcal{H}}}{\Gamma(\delta)} \max_{t \in [0, T]} \left| \int_0^{t_1} (t_1 - \alpha)^{\delta-1} d\alpha - \int_0^{t_2} (t_2 - \alpha)^{\delta-1} d\alpha \right|, \\ &\leq \frac{\mathcal{L}_{\mathcal{H}}}{\Gamma(\delta + 1)} \max_{t \in [0, T]} |t_1^\delta - t_2^\delta| \rightarrow 0 \text{ as } t_1 \rightarrow t_2. \end{aligned}$$

Thus, \mathcal{Z} is equicontinuous. \mathcal{Z} is compact, and hence, it is completely continuous because of the continuousness and boundedness, it. Let $\Psi = \{U \in \mathcal{A} : U = \rho \mathcal{Z}(U), \rho \in [0, 1]\}$, we need to confirm that Ψ is bounded. Suppose $U \in \Psi$, say S , then for $t \in [0, T]$, we have:

$$\begin{aligned} \|S\| &= \max_{t \in [0, T]} \left\{ \frac{\rho}{\Gamma(\delta)} \int_0^t (t - \alpha)^{\delta-1} \mathcal{H}(\alpha, S(\alpha)) d\alpha \right\} \\ &\leq \frac{\mathcal{L}_{\mathcal{H}}}{\Gamma(\delta)} \max_{T \in [0, T]} \int_0^t (t - \alpha)^{\delta-1} d\alpha \leq \frac{T^\delta \mathcal{L}_{\mathcal{H}}}{\Gamma(\delta + 1)}. \end{aligned}$$

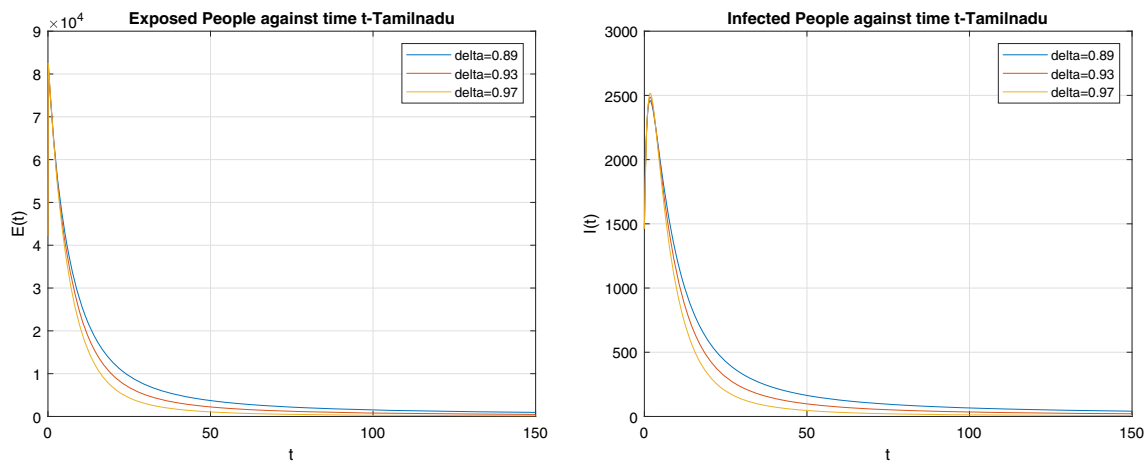


Fig. 2 Exposed $E(t)$ and infected $I(t)$ people against time t in the data of Tamilnadu

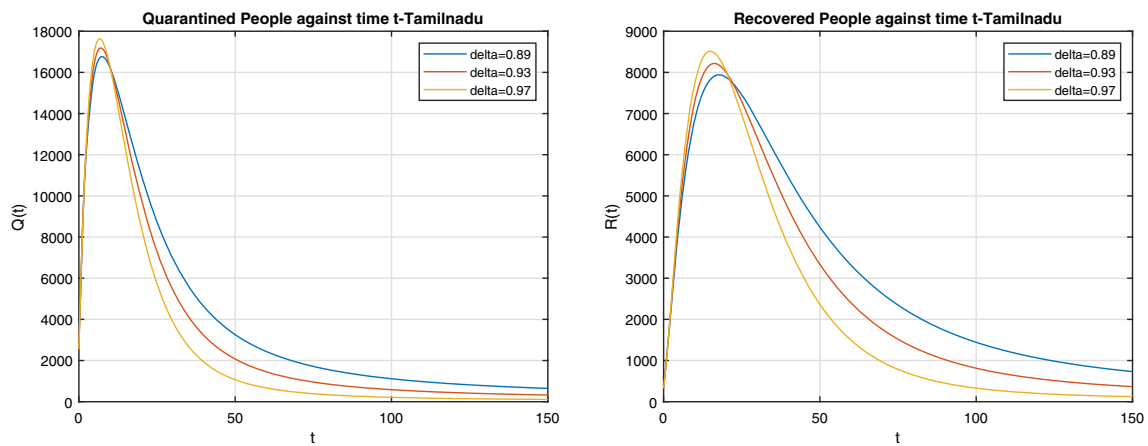


Fig. 3 Isolated $Q(t)$ and recovered $R(t)$ people against time t in the data of Tamilnadu

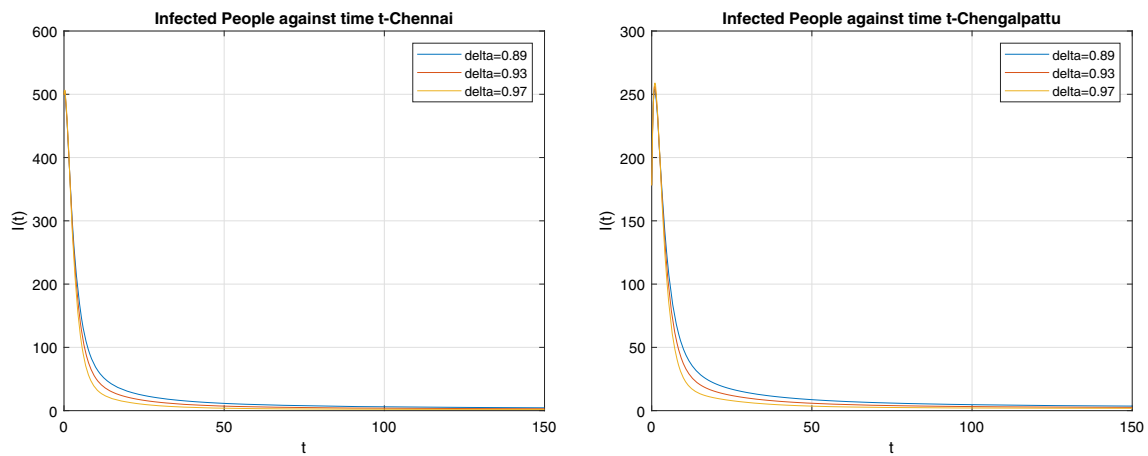


Fig. 4 The infected $I(t)$ against time t for the districts Chennai and Chengalpattu of Tamilnadu

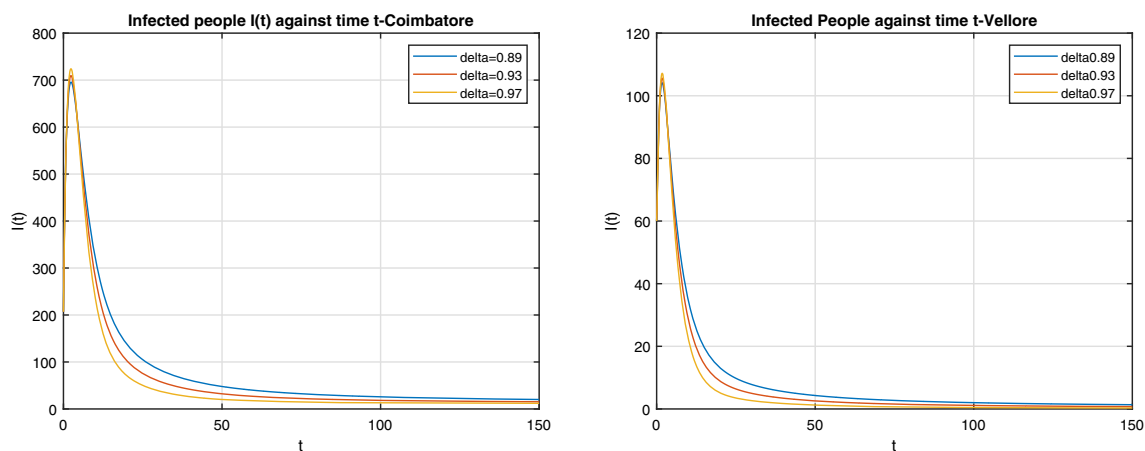


Fig. 5 The infected $I(t)$ against time t for the districts Coimbatore and Vellore of Tamilnadu

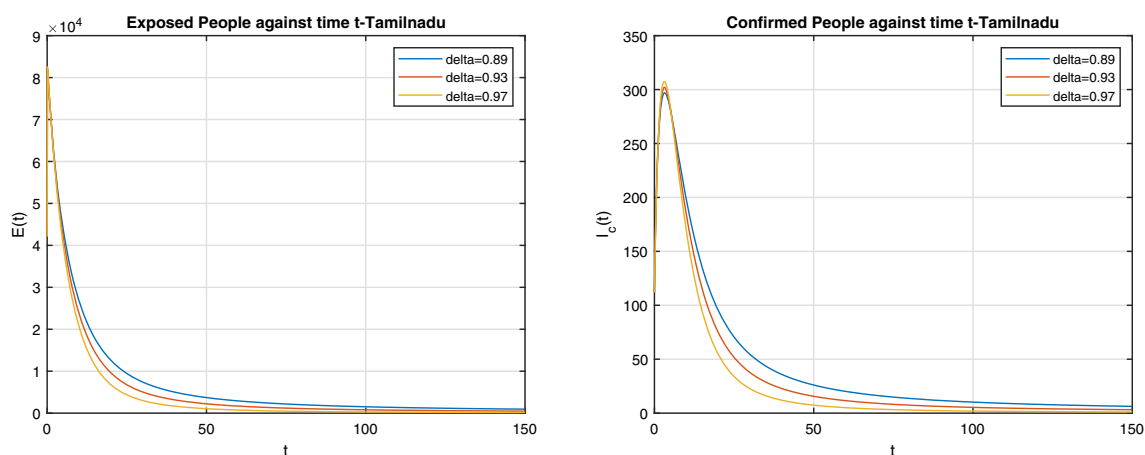


Fig. 6 Exposed $E(t)$ and confirmed $I_c(t)$ people against time t

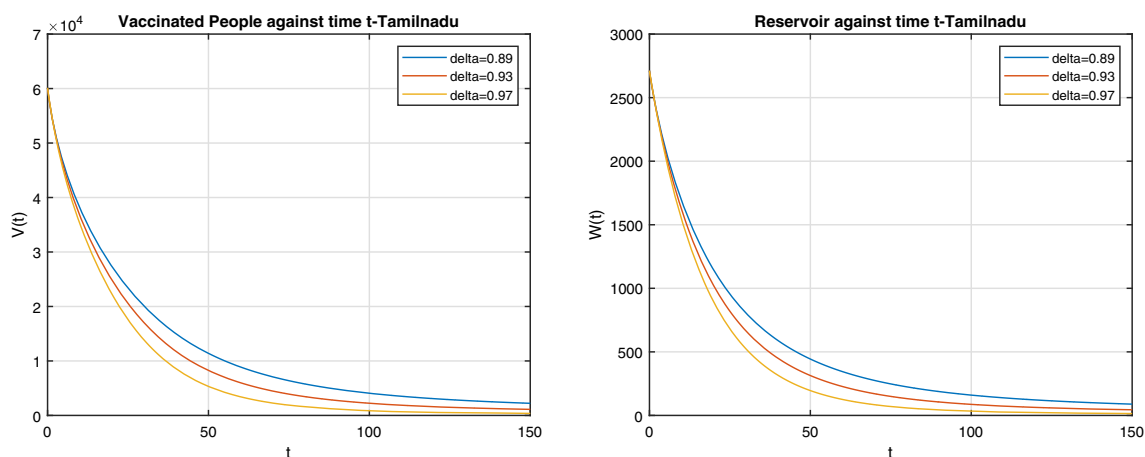


Fig. 7 Vaccinated $V(t)$ and reservoir $W(t)$ people against time t

Thus, the operator is completely continuous. The set Ψ is also bounded. Therefore, \mathcal{Z} has at least one fixed point [39]. So, the considered system (4) has the same number of solutions. \square

Theorem 7 If $\frac{\beta_i}{\Gamma(\delta)}t < 1$, for $i = 1, 2, \dots, 8$, then the system (4) has a unique solution.

Proof Assume that $\{S_v(t), E_v(t), I_v(t), Q_1(t), I_{c_v}(t), R_v(t), V_v(t), W_v(t)\}$ is another set of solutions of the sys-

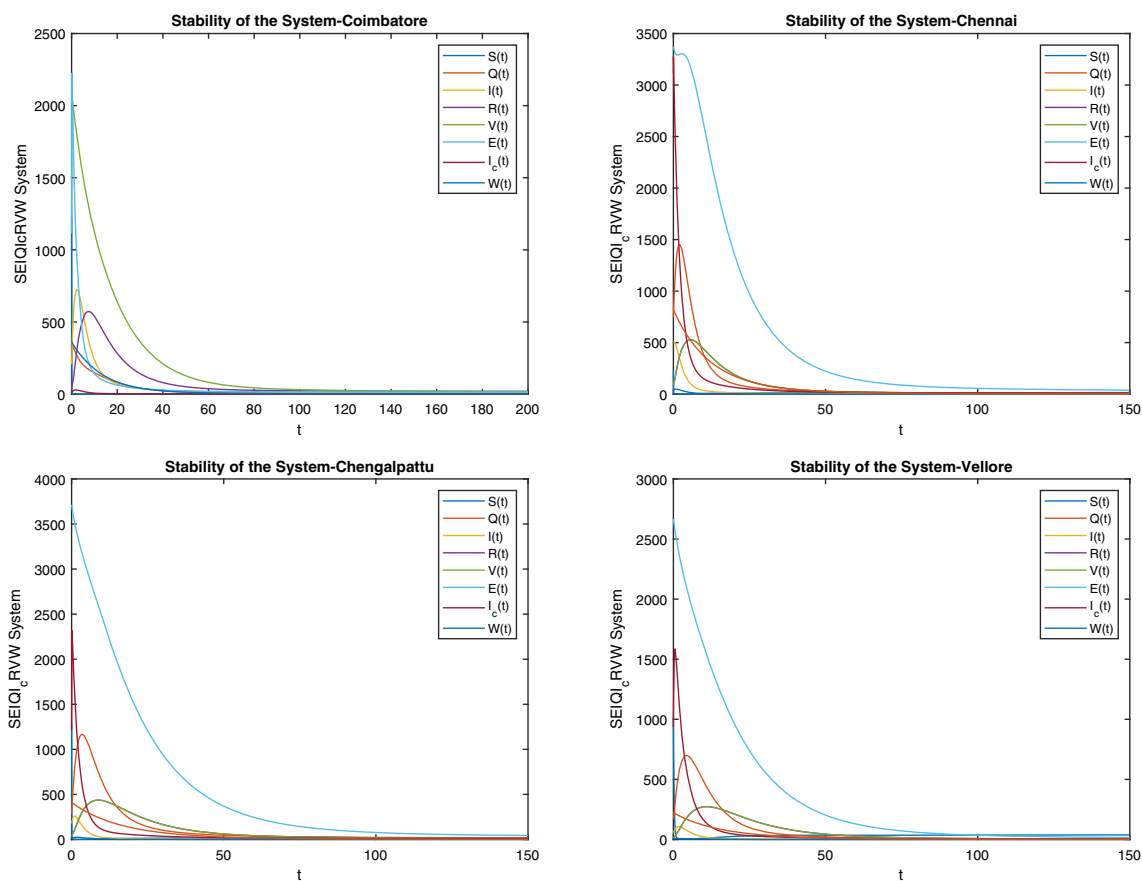


Fig. 8 Stability of the given Omicron system against time t in the four districts Coimbatore, Chennai, Chengalpattu and Vellore of Tamilnadu

Table 2 Omicron status across the districts of Tamilnadu as on March 11, 2022

Descriptions	Tamilnadu	Chennai	Coimbatore	Chengalpattu	Vellore
Positive cases	3,451,710	750,606	329,778	235,295	54,943
Discharged	3,412,226	750,520	329,737	235,260	54,930
Deaths	38,023	48	51	5	2321
Active cases	1461	499	207	178	60
Positive cases on 11	112	42	13	12	4
Recovered on 11	327	86	41	35	13
Vaccinated on 11	60,128	3373	2083	3713	2667

tem (4); then,

$$\begin{aligned} \|S(t) - S_v(t)\| &= \frac{1}{\Gamma(\delta)} \int_0^t [\mathcal{H}(\alpha, S) - \mathcal{H}(\alpha, S_v)] \alpha \\ &= \frac{\beta_1}{\Gamma(\delta)} t \|S(t) - S_v(t)\|. \end{aligned}$$

Thus,

$$\left(1 - \frac{\beta_1}{\Gamma(\delta)} t\right) \|S(t) - S_1(t)\| \leq 0. \tag{21}$$

Since $\frac{\beta_i}{\Gamma(\delta)} t < 1$ for $i = 1, (21)$ becomes $\|S(t) - S_v(t)\| = 0$.

Hence, $S(t) = S_v(t)$. Similarly, for $i = 2, 3, \dots, 8$, we can get $E(t) = E_v(t); I(t) = I_v(t); Q(t) = Q_v(t); I_c(t) = I_{c_v}(t); R(t) = R_v(t); V(t) = V_v(t); W(t) = W_v(t)$. Hence, the system (4) has a unique solution. \square

4 Numerical analysis

In the second wave of the corona virus, India experienced a high infection rate. We have gathered data from Tamilnadu,

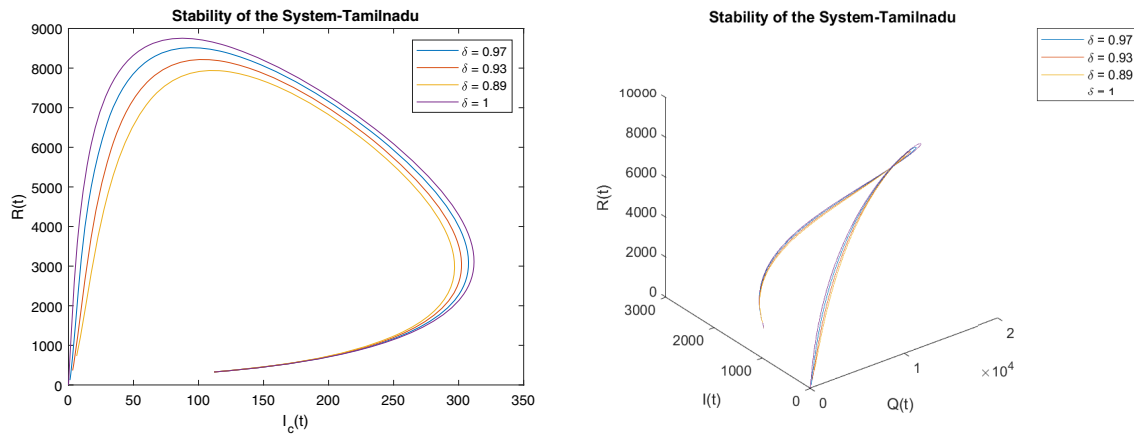


Fig. 9 Infected, isolated and recovered individuals against time t in Tamilnadu

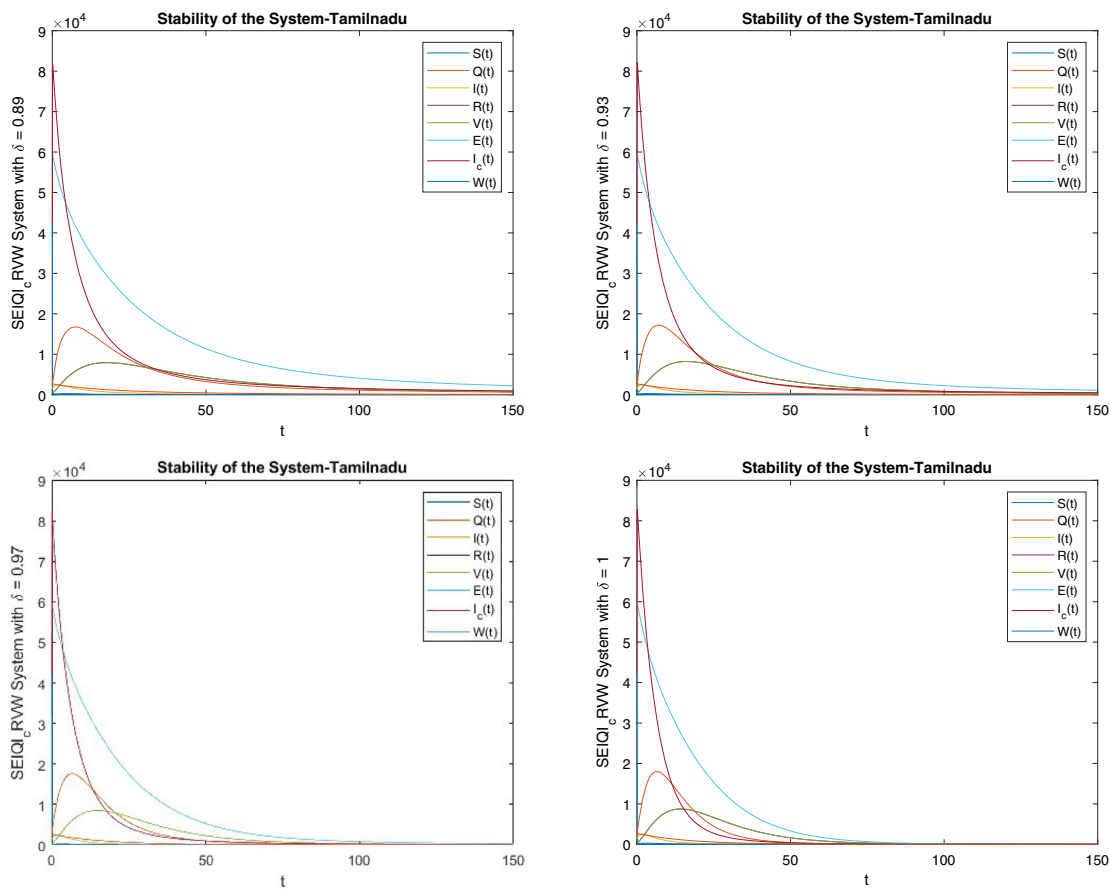


Fig. 10 Stability condition of the Tamilnadu against time t with various δ

India for our study [40]. The first case of the Omicron strain of SARS-CoV-2 by a traveler from another nation was reported in Tamil Nadu on Wednesday, December 15th. Tamil Nadu has been infected with the highly transmissible and fast-spreading form of SARS-CoV-2 just three weeks after the first confirmed Omicron case was reported.

On December 29, when 739 people tested positive, the number of daily cases began to rise, quickly reaching over 10,000 on January 8. In the initial wave, it took 58 days for the daily count in the state to rise from 1000 to nearly 7000 cases. It took 26 days for the cases in the second wave to rise from 1000 to over 7000. The number of cases reached 36,000 after another 38 days. The daily instances, on the other hand,

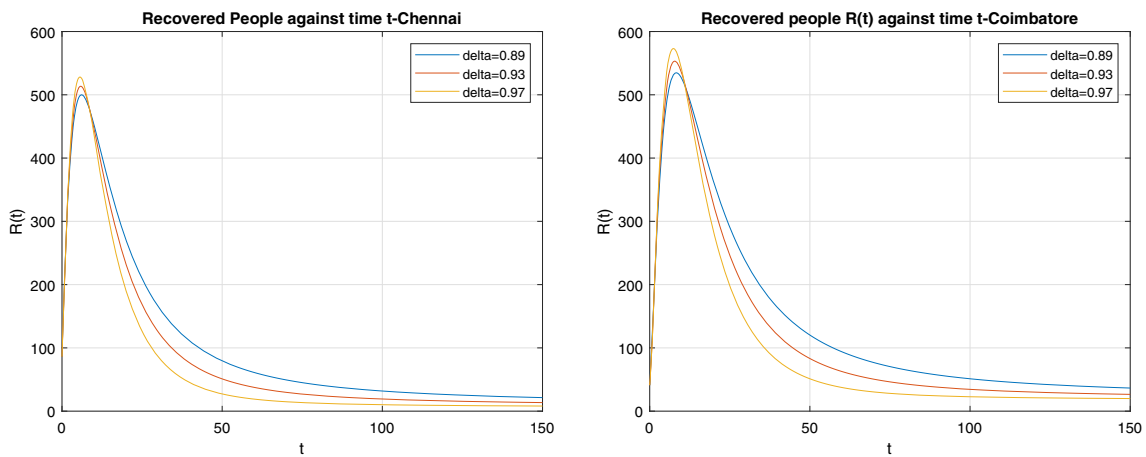


Fig. 11 Recovered range about various reproduction numbers 0.66, 0.92, 0.63 and 0.06 in Chennai and Coimbatore districts

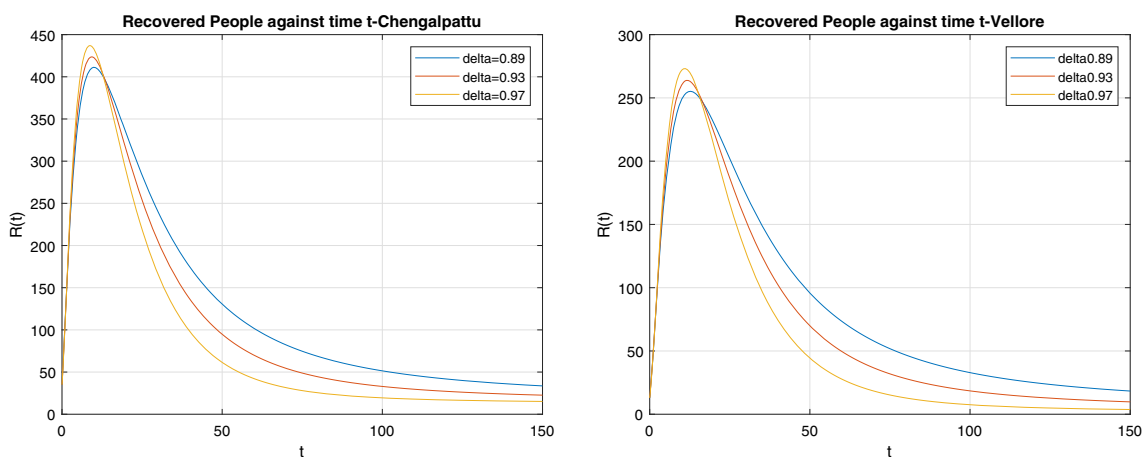


Fig. 12 Recovered range about various reproduction numbers 0.66, 0.92, 0.63 and 0.06 in Chengalpattu and Vellore districts

have only taken 7 days to increase from 1000 to 7000. Chennai has quickly become a hotspot, fueling the growth. Due to the high caseload, Chengalpattu, Coimbatore and Vellore are the other areas of concern. Whole genome sequencing revealed that 99.9% of the samples were of the Delta variant in the last three months. Earlier, it was 65% Omicron and 35% Delta due to the fast changing situation. According to a statement released by the Tamil Nadu public health department, the BA.2 sub variation of Omicron was found in 18.4% of the samples sequenced in the state from January to March 2022. On March 11th, the state of Tamilnadu achieves a safe position against the propagation of Omicron viruses and a death rate of zero [40–43]. Mathematica is used to calculate the numerical solution using Adams–Bashforth–Moulton scheme. The values of the variables and parameters are listed in Tables 1 and 2.

The solution for (4) demonstrates that it is unstable locally and will never become stable when $R_0 > 1$, as shown in the figures. The steady state solution becomes stable when the contact rate is controlled and the vaccination class is

increased when $R_0 < 1$. We conclude from all of the data that if the number of isolated, recovered, and vaccinated people increases, the host community will be safe from the Omicron variant. We also discovered that if the intercessions are strictly followed, the spread of the second wave of SARS Cov-2 Omicron variant is reduced.

Figures 2 and 3 describe the visualization of the impact of Omicron variant in the susceptible individual, infected individual, isolated individual and recovered individual against time t in the overall state of Tamilnadu.

Figures 4 and 5 illustrate the infected individuals against time t in Tamilnadu’s four districts. Because the government increased the number of quarantine and vaccination facilities, the number of infected people has decreased significantly.

Figures 6 and 7 describe the exposed, confirmed, vaccinated and the reservoir rates of the host of human population, respectively, against the time t in the state of Tamilnadu. Figs. 2 and 6 show how persons in Tamilnadu were infected and confirmed with the Omicron variant in the beginning and recovered by the end of March 11th, 2022. It is obvious

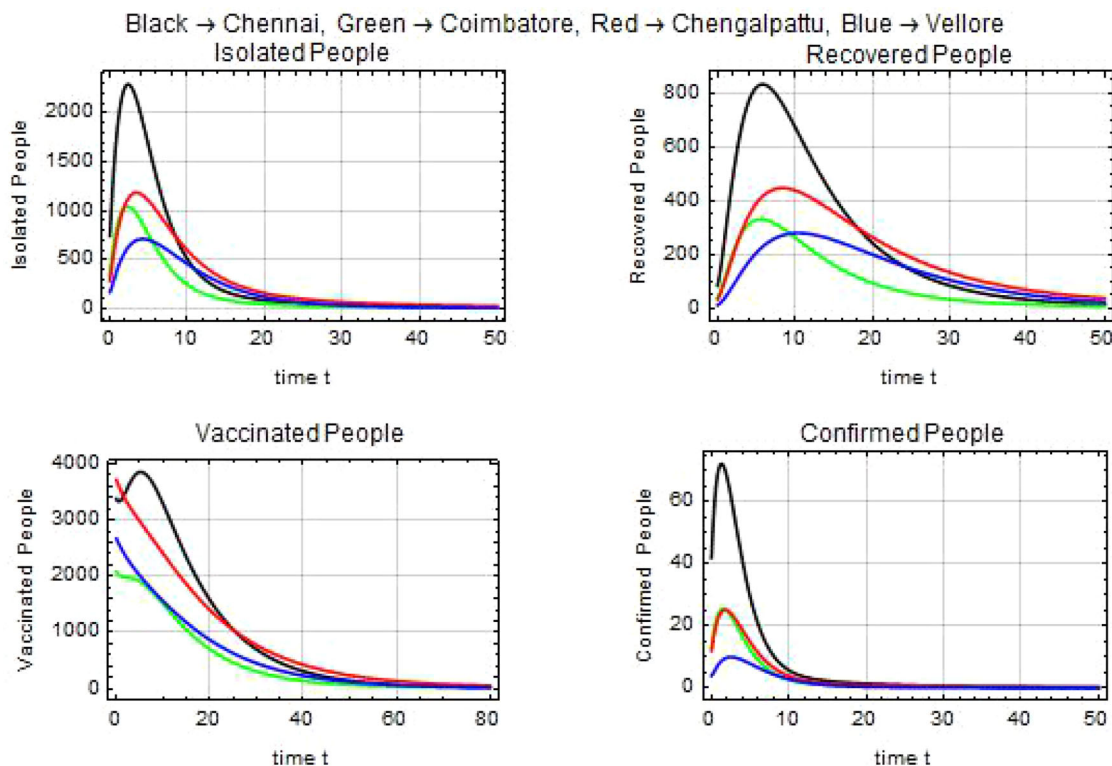


Fig. 13 Isolated, confirmed, recovered and vaccinated people of four districts for the given data when $\delta = 1$

from Figs. 2 and 6 that once the exposed population increases, all other compartments increase as well. Due to the loss of immunity, we see a newfound availability of susceptible individuals after nearly 50 days in our model. In addition, if there is an increase in isolated and vaccinated classes, a disease-free field will exist after 80 days when $\delta = 0.97$.

The stability of the Omicron mathematical model for the four districts of Chennai, Coimbatore, Chengalpattu and Vellore is depicted in Fig. 8. During the Omicron period, which runs from December 25th to March 11th, 2022, the people of these four districts have a high rate of illness. When people were vaccinated according to government instructions, the infection rate progressively decreased to a low level. From the fractional-order simulations, we notice that according to the various fractional-order cases, the infection can take more time to disappear from the population compared to integer-order observations. The biological reason for such delay in disease control can be not following the quarantine, not taking the vaccine, or not using basic protective controls. Integer-order derivatives can't capture such effects.

According to Table 2, as of March 11, the number of infected people in these four districts has decreased to 42, 13, 12 and 4 in the districts of Chennai, Coimbatore, Chengalpattu and Vellore, respectively, based on RT PCR sample tests 3233, 1233, 1286 and 1017, with no death.

Figure 9 describes the relation between the rates of infected, isolated and recovered people in the infection period of Omicron in Tamilnadu state.

Figure 10 demonstrates the stability graph representation of the constructed model in the host population in Tamilnadu with various order of δ . Figure 10 shows that when the Omicron variant was first discovered, its spread was rapid, and when the government implemented quarantine and vaccination at a high rate, the variant's spread was reduced to a safe level. On March 11, 2022, the state of Tamilnadu discovered that no one had caused the death of Omicron. COVID-19 vaccinations helped people avoid infection with the SARS CoV-2 Omicron variant.

Figures 11 and 12 describe the recovered rate of the four districts Chennai, Coimbatore, Chengalpattu and Vellore according to the corresponding reproduction numbers 0.66, 0.92, 0.63 and 0.06.

Figure 13 describes the isolated, confirmed, recovered and vaccinated individuals rates of the four districts Chennai, Coimbatore, Chengalpattu and Vellore.

We can observe from Fig. 13 and Table 3 that the infected rate decreases and the recovered rate increased after a rapid spread over a short time with the reproduction number $R_0 < 1$. As a result, the system in the four districts, as well as the entire state of Tamilnadu, is stable.

Table 3 Values of the variables

Parameters	Tamilnadu	Chennai	Coimbatore	Chengalpattu	Vellore
$S(0)$	42,241	3233	1233	1286	1017
$E(0)$	42,132	3118	1114	1215	936
$I(0)$	1461	499	207	178	60
$Q(0)$	2542	744	353	286	168
$I_c(0)$	112	42	13	12	4
$R(0)$	327	86	41	35	13
$V(0)$	60,128	3373	2083	3713	2667
$W(0)$	2712	821	365	412	224
Λ	5	5	5	5	3
μ_s	0.0346	0.1543	0.1679	0.1384	0.0590
α_v	0.0054	0.0255	0.0197	0.0094	0.0049
δ_n	0.0650	0.0870	0.0900	0.0650	0.0690
ρ_r	0.0077	0.0266	0.0333	0.0272	0.0128
ρ_v	0.0070	0.0096	0.0059	0.0035	0.0038
δ_e	0.0006	0.0002	0.0002	0.0001	0.0422
δ_c	0.0027	0.0135	0.0117	0.0099	0.0043
ν_r	0.2238	0.1723	0.1981	0.1966	0.2167
τ	0.5747	0.6707	0.5864	0.6224	0.3571
ζ_q	0.0441	0.0565	0.0368	0.0420	0.0238
η_v	0.0423	0.2206	0.1695	0.0770	0.0630
γ_c	0.3425	0.4884	0.3171	0.3429	0.3077
γ_i	0.0347	0.1600	0.1858	0.1465	0.0641
γ_r	0.0447	0.0580	0.0505	0.0509	0.0462
ζ_w	0.0004	0.0005	0.0004	0.0003	0.0002
ω_c	0.0054	0.0061	0.0057	0.0043	0.0027
k	0.0603	0.2386	0.3169	0.2354	0.1795
R_0	0.0131	0.6634	0.9221	0.6330	0.0597

5 Conclusions

In this research, a novel epidemic fractional-order mathematical model for Omicron B.1.1.529 SARS-Cov-2 Variant was developed with eight compartments and important parameters. The data acquired from Tamil Nadu and several of its districts, together with our mathematical model, suggest that the Omicron variant infection has stabilized after a few months. This model outperforms other mathematical models by taking into account the nonlinear force of quarantine, vaccine, infection and care, as well as the right inclusion of valuable parameters. The principles of reproduction number calculated with this model are an outbreak threshold that determined whether or not the disease would go further in Tamilnadu where $R_0 < 1$. The fundamentals of positivity, boundedness and the existence of unique solutions have been examined and validated. There are infection-free steady-state solutions that are asymptotically stable when $R_0 < 1$. Finally, the current Omicron variant pandemic data of Tamilnadu, India, are validated. In the fractional-order

simulations, we have observed the possibility of delay in the decrement of Omicron cases. The biological reason for such delay in disease control can be not following the quarantine, not taking the vaccine, or not using basic protective controls. Such effects could not be captured by using integer-order derivatives.

In the future, the proposed model can be considered to forecast disease outbreaks for any other real data. Also, the same model can be generalized by using several other fractional derivatives.

Acknowledgements The first author is partially supported by the University Research Fellowship (PU/AD-3/URF/ 21F37237/2021 dated 09.11.2021) of Periyar University, Salem. The second author is supported by the fund for improvement of Science and Technology Infrastructure (FIST) of DST (SR/FST/MSI-115/2016).

Author Contributions SD contributed to conceptualization, visualization, software, resources, formal analysis, investigation, and writing—original draft. SP performed investigation, supervision, formal analysis, and writing—review and editing. PK contributed to investigation, resources, visualization, and writing—review and editing.

Funding Not applicable.

Availability of data and materials The data used in this research are available/mentioned within the manuscript.

Declarations

Conflict of interest The authors declare that they have no competing interests.

References

- Ojo MM, Peter OJ, Goufo EFD, Nisar KS (2023) A mathematical model for the co-dynamics of COVID-19 and tuberculosis. *Math Comput Simul.* <https://doi.org/10.1016/j.matcom.2023.01.014>
- Kammegne B, Oshinubi K, Babasola O, Peter OJ, Longe OB, Ogunrinde RB, Demongeot J (2023) Mathematical modelling of the spatial distribution of a COVID-19 outbreak with vaccination using diffusion equation. *Pathogens* 12(1):88
- Babasola O, Kayode O, Peter OJ, Onwuegbuche FC, Oguntolu FA (2022) Time-delayed modelling of the COVID-19 dynamics with a convex incidence rate. *Inform Med Unlock* 35:101124
- Ayoade AA, Ikpechukwu PA, Thota S, Peter OJ (2022) Modelling the effect of quarantine and hospitalization on the spread of COVID-19 during the toughest period of the pandemic. *J Mahani Math Res* 12:339–361
- Peter OJ, Qureshi S, Yusuf A, Al-Shomrani M, Idowu AA (2021) A new mathematical model of COVID-19 using real data from Pakistan. *Results Phys* 24:104098
- Abioye AI, Peter OJ, Ogunseye HA, Oguntolu FA, Oshinubi K, Ibrahim AA, Khan I (2021) Mathematical model of COVID-19 in Nigeria with optimal control. *Results Phys* 28:104598
- Chatzarakis GE et al (2022) A dynamic SI_qIRV mathematical model with non-linear force of isolation, infection and cure. *Nonauton Dyn Syst* 9(1):56–67. <https://doi.org/10.1515/msds-2022-0145>
- Oke MO et al (2019) Mathematical modeling and stability analysis of a SIRV epidemic model with non-linear force of infection and treatment. *Commun Appl Math* 10(4):717–731
- Rao JPRS, Kumar MN (2015) A dynamic model for infectious diseases: the role of vaccination and treatment. *Chaos Solitons Fractals* 75:34–49. <https://doi.org/10.1016/j.chaos.2015.02.004>
- Beretta E, Cappasso V (1986) On the general structure of epidemic system: global stability. *Comput Math Appl* 12:677–694. [https://doi.org/10.1016/0898-1221\(86\)90054-4](https://doi.org/10.1016/0898-1221(86)90054-4)
- Yang W et al (2010) Global analysis for a general epidemiological model with vaccination and varying population. *J Math Anal Appl* 372:208–223. <https://doi.org/10.1016/j.jmaa.2010.07.017>
- Kim BN et al (2020) Mathematical model of COVID-19 transmission dynamics in South Korea: the impacts of travel. *Soc Distancing Early Detect Process* 8:1304. <https://doi.org/10.3390/pr8101304>
- Deborah DO (2020) Mathematical model for the transmission of Covid-19 with nonlinear forces of infection and the need for prevention measure in Nigeria. *J Inf Dis Epidemiol* 6(5):1–12. <https://doi.org/10.23937/2474-3658/1510158>
- Tomochi M, Kono M (2021) A mathematical model for COVID-19 pandemic-SIIR model: effects of asymptomatic individuals. *J Gen Fam Med* 22:5–14. <https://doi.org/10.1002/jgf2.382>
- Biswas SK et al (2020) Covid-19 pandemic in India: a mathematical model study. *Nonlinear Dyn.* <https://doi.org/10.1007/s11071-020-05958-z>
- Muniyappan A et al (2022) Stability and numerical solutions of second wave mathematical modeling on COVID-19 and Omicron outbreak strategy of pandemic: analytical and error analysis of approximate series solutions by using HPM. *Mathematics* 343:10. <https://doi.org/10.3390/math10030343>
- Wang B-G et al (2023) A mathematical model reveals the influence of NPIs and vaccination on SARS-CoV-2 Omicron variant. *Res Sq.* <https://doi.org/10.21203/rs.3.rs-1324280/v1>
- Ozkose F et al (2022) Fractional order modelling of Omicron SARS-CoV-2 variant containing heart attack effect using real data from the United Kingdom. *Chaos Solitons Fractals* 157:111954. <https://doi.org/10.1016/j.chaos.2022.111954>
- Li GH, Zhang YX (2017) Dynamic behavior of a modified SIR model in epidemic diseases using non linear incidence rate and treatment. *PLoS ONE* 12(4):e0175789. <https://doi.org/10.1371/journal.pone.0175789>
- Riyapan P et al (2021) A mathematical model of COVID-19 pandemic: a case study of Bangkok, Thailand. *Comput Math Models Med* 6664483:1–11
- Peter OJ, Yusuf A, Ojo MM, Kumar S, Kumari N, Oguntolu FA (2022) A mathematical model analysis of meningitis with treatment and vaccination in fractional derivatives. *Int J Appl Comput Math* 8(3):117
- Peter OJ, Yusuf A, Oshinubi K, Oguntolu FA, Lawal JO, Abioye AI, Ayoola TA (2021) Fractional order of pneumococcal pneumonia infection model with Caputo Fabrizio operator. *Results Phys* 29:104581
- Peter OJ (2020) Transmission dynamics of fractional order Brucellosis model using caputo-fabrizio operator. *Int J Differ Equ* 2020:1–11
- Peter OJ, Shaikh AS, Ibrahim MO, Nisar KS, Baleanu D, Khan I, Abioye AI (2021) Analysis and dynamics of fractional order mathematical model of COVID-19 in Nigeria using Atangana–Baleanu operator. *Comput Mater Contin* 66(2):1823–1848
- Kumar P, Erturk VS, Govindaraj V, Inc M, Abboubakar H, Nisar KS (2022) Dynamics of COVID-19 epidemic via two different fractional derivatives. *Int J Model Simul Sci Comput*
- Owoyemi AE, Sulaiman IM, Kumar P, Govindaraj V, Mamat M (2022) Some novel mathematical analysis on the fractional-order 2019-nCoV dynamical model. *Math Methods Appl Sci* 46:4466–4474
- Vellappandi M, Kumar P, Govindaraj V (2022) A case study of 2019-nCoV in Russia using integer and fractional order derivatives. *Math Methods Appl Sci.* <https://doi.org/10.1002/mma.8736>
- Kumar P, Erturk VS, Nisar KS, Jamshe W, Mohamed MS (2022) Fractional dynamics of 2019-nCoV in Spain at different transmission rate with an idea of optimal control problem formulation. *Alexand Eng J* 61(3):2204–2219
- Kumar P, Erturk VS, Murillo-Arcila M, Banerjee R, Manickam A (2021) A case study of 2019-nCoV cases in Argentina with the real data based on daily cases from March 03, 2020 to March 29, 2021 using classical and fractional derivatives. *Adv Differ Equ* 2021(1):1–21
- Zeb A, Kumar P, Erturk VS, Sitthiwirattam T (2022) A new study on two different vaccinated fractional-order COVID-19 models via numerical algorithms. *J King Saud Univ Sci* 34(4):101914
- Chen H, Cui Y (2022) Existence of extremal solutions for a fractional compartment model. *J Appl Math Comput* 68:941–951. <https://doi.org/10.1007/s12190-021-01556-3>
- Hikal MM et al (2022) Stability analysis of COVID-19 model with fractional-order derivative and a delay in implementing the quarantine strategy. *J Appl Math Comput* 68:295–321. <https://doi.org/10.1007/s12190-021-01515-y>
- Kumar P, Suat Erturk V (2021) A case study of COVID-19 epidemic in India via new generalised Caputo type fractional derivatives. *Math Methods Appl Sci.* <https://doi.org/10.1002/mma.7284>

34. Ahmad S et al (2020) Fractional order mathematical modeling of COVID-19 transmission. *Chaos Solitons Fractals* 139:110256
35. Rezapour S et al (2020) SEIR epidemic model for Covid-19 transmission by Caputo derivative of fractional order. *Adv Differ Equ.* <https://doi.org/10.1186/epjp/s13662-020-02952-y>
36. Podlubny I (1999) *Fractional differential equations, mathematics in science and engineering.* Academic Press, New York
37. Diekmann O et al (1990) On the definition and computation of the basic reproduction number R_0 in models for infectious disease. *J Math Biol* 28:365–382. <https://doi.org/10.1007/BF00178324>
38. Van den Driessche P, Watmough J (2002) Reproduction Number and sub threshold epidemic equilibrium for compartmental models for disease transmission. *Math Biosci* 180:29–48. [https://doi.org/10.1016/S0025-5564\(02\)00108-6](https://doi.org/10.1016/S0025-5564(02)00108-6)
39. Granas A, Dugundji J (2015) *Fixed point theory.* Springer, New York
40. <https://www.mygov.in/covid-19>
41. <https://www.mohfw.in/covid-19> (as on March 11)
42. <https://www.tn.data.gov.in/catalog/covid-19>
43. <https://covid19.who.int/region/searo/country/in>

Springer Nature or its licensor (e.g. a society or other partner) holds exclusive rights to this article under a publishing agreement with the author(s) or other rightsholder(s); author self-archiving of the accepted manuscript version of this article is solely governed by the terms of such publishing agreement and applicable law.